ChemPubSoc Europe

DOI: 10.1002/cctc.201300375

One-Step Room-Temperature Synthesis of [Al]MCM-41 Materials for the Catalytic Conversion of Phenylglyoxal to Ethylmandelate

Zichun Wang,[a] Yijiao Jiang,[b] Rafal Rachwalik,[c] Zhongwen Liu,[a] Jeffrey Shi,[a] Michael Hunger,*[d] and Jun Huang*[a]

Mesoporous [Al]MCM-41 materials with n_{Si}/n_{Al} ratios of 15 to 50 suitable for the direct catalytic conversion of phenylglyoxal to ethylmandelate have been successfully synthesized at room temperature within 1 h. The surface areas and pore sizes of the obtained [Al]MCM-41 materials are in the ranges of 1005–1246 $m^2 g^{-1}$ and 3.44–3.99 nm, respectively, for the different n_{Si}/n_{Al} ratios. For all [Al]MCM-41 catalysts, most of the Al species were tetrahedrally coordinated with Si in the next coordination sphere of atoms. ^1H and ^{13}C magic-angle spinning NMR spectroscopic investigations indicated that the acid strength of the SiOH groups on these [Al]MCM-41 catalysts and the density of these surface sites are enhanced with increasing Al content in the synthesis gels. These surface sites with enhanced acid strength were found to be catalytically active sites for phenylglyoxal conversion. The [Al]MCM-41 material with $n_{Si}/n_{Al}=15$ showed the highest phenylglyoxal conversion (93.4%) and selectivity to ethylmandelate (96.9%), whereas the [Al]MCM-41 material with $n_{Si}/n_{Al}=50$ reached the highest turnover frequency (TOF = 99.3 h^{-1}). This is a much better catalytic performance than that of a dealuminated zeolite Y (TOF = 1.7 h^{-1}) used as a reference catalyst, which is explained by lower reactant transport limitations in mesoporous materials than that in the microporous zeolite.

Introduction

Mesoporous MCM-41 materials are silica-based systems with hexagonally arranged mesopores with long-range order, which were initially developed in 1992.[1] Generally, the ordered mesopores are formed through the condensation of silicates around the self-assembled micelles by surfactant molecules or through liquid-crystal phases influenced by the silicate. During the past decades, numerous routes for the synthesis of MCM-41 materials have been developed.[1b,2] With modification of the synthesis conditions, such as the type of solvents, silica sources, addition of other metal species (e.g., Al), surfactant type and relative concentration, pH value, synthesis temperature, aging and drying conditions, etc., the morphology and catalytic properties of the obtained MCM-41 materials can be controlled.[2a,3] Among them, the direct room-temperature synthesis of siliceous MCM-41[3c,f,h,4] has drawn great interest as it is a rapid method under mild conditions with less energy and time consumed compared with classic hydrothermal synthesis (heating normally required at 60–150 °C for 1–6 d).[1,5]

Huo et al.[6] synthesized mesoporous silica spheres by using different silica sources under basic conditions with stirring for 15–30 h at room temperature. They found that lower alkoxysilanes, such as tetramethyl orthosilicate (TMOS) and tetraethyl orthosilicate (TEOS), yielded only small MCM-41 particles, whereas higher alkoxysilanes, such as tetrabutyl orthosilicate (TBOS), led to larger MCM-41 spheres. These spheres were obtained at a low stirring speed (< 200 rpm), whereas the formation of small particles occurred at a high stirring speed (>450 rpm). Cai et al.[3c] and Grun et al.[3h] synthesized siliceous MCM-41 particles in a diluted solution of surfactants with tetraethoxysilane under basic conditions at room temperature with stirring for 2 h. The resulting particle size was in the range of micrometers (1 μm) to nanometers (100 nm) controlled by using different basic additives ($NaOH/NH_4OH$)[3c] and surfactants (*n*-hexadecyltrimethylammonium bromide and *n*-hexadecylpyridiniumchloride monohydrate).[3h] Recently, Pescarmona and co-workers[3a,7] synthesized [Ti]MCM-41 materials with particle sizes of 80–160 nm by using TEOS, cetyltrimethylammonium bromide (CTAB), NaOH, and titanium(IV) isopropoxide with stirring at room temperature for 2 h and found that

[a] Z. Wang, Dr. Z. Liu, Dr. J. Shi, Dr. J. Huang
Laboratory for Catalysis Engineering
School of Chemical and Biomolecular Engineering
The University of Sydney
NSW 2006 (Australia)
Fax: (+61) 2-9351-2854
E-mail: jun.huang@sydney.edu.au

[b] Dr. Y. Jiang
School of Chemical Engineering
The University of New South Wales
NSW 2052 (Australia)

[c] Dr. R. Rachwalik
Institute of Organic Chemistry and Technology
Cracow University of Technology
31-155 Kraków (Poland)

[d] Prof. Dr. M. Hunger
Institute of Chemical Technology
University of Stuttgart
70550 Stuttgart (Germany)
Fax: (+49) 711-685-64081
E-mail: michael.hunger@itc.uni-stuttgart.de

these are suitable catalysts for the epoxidation of cyclohexene with H_2O_2. In addition, [Al]MCM-41 materials were synthesized under similar conditions by using a mixture of TEOS and aluminum isopropoxide (AIP) as precursors under basic (aqueous ammonia) or acidic (HCl) conditions.[8]

MCM-41 materials with and without doping with metal species (B, Ga, Ti, Al, and Fe) have been widely utilized in heterogeneous catalysis, drug delivery, and adsorption technologies.[1,2b,9] Most of these applications require materials with well-defined morphologies, adsorption properties, and acidity.[1b,2b,3a,b,9,10] Therefore, the synthesis of MCM-41 materials with the desired properties has attracted much attention. One of the most important modifications of MCM-41 materials is the incorporation of Al into the silica framework to lead to the formation of surface SiOH groups with enhanced acid strength. These acidic [Al]MCM-41 materials are promising as solid-acid catalysts as well as supports of nanometal catalysts for bifunctional catalysis because of their better reactant/product diffusion properties for big molecules inside the mesopores[8a,11] compared with widely used microporous zeolites. Therefore, the incorporation of Al into the framework of mesoporous [Al]MCM-41 materials is a convenient method to tune the Brønsted acidity for desired catalytic reactions, and in the present work, these catalysts have been prepared by a rapid, one-step, room-temperature synthetic route.

For the development of green processes in the chemical industry, an increasing number of solid acids have replaced liquid catalysts. In fine chemistry for example, solid acids were recently applied in the conversion of α-keto aldehyde to α-hydroxyl carboxylates in alcohols.[12] In this case, phenylglyoxal (PG) is converted in ethanol to yield ethylmandelate (EM), which is an essential chemical in the pharmaceutical and fine-chemical industries.[13] Recently, an EM yield of 95% with a selectivity of 97% was obtained on a USY zeolite.[12c]

In this work, we present a one-step method for the synthesis of [Si]MCM-41 and [Al]MCM-41 materials with different n_{Si}/n_{Al} ratios at room temperature. These materials were characterized by XRD, N_2 adsorption–desorption, and electron microscopy for their long-range order, texture, and morphology. As a powerful technique for the characterization of aluminosilicates,[14] solid-state NMR spectroscopy was used for the investigation of the local structure of the [Al]MCM-41 framework and the surface acid sites. Finally, the conversion of PG to EM was employed on [Al]MCM-41 catalysts as a test reaction.

Results and Discussion

Characterization of textural and morphological properties

XRD patterns recorded in the small-angle region ($2\theta = 1.5$–10°) of the MCM-41 materials with different n_{Si}/n_{Al} ratios are shown in Figure 1. A typical pattern that indicates a hexagonal framework was observed for [Si]MCM-41 in Figure 1a as evidenced by the strong (100) reflections at low angles and weak (110), (200), and (210) reflections at 4.1, 4.7, and 6.3°, respectively. These reflections are a result of the long-range order of the MCM-41 materials.[15] With an increasing Al content, the weak

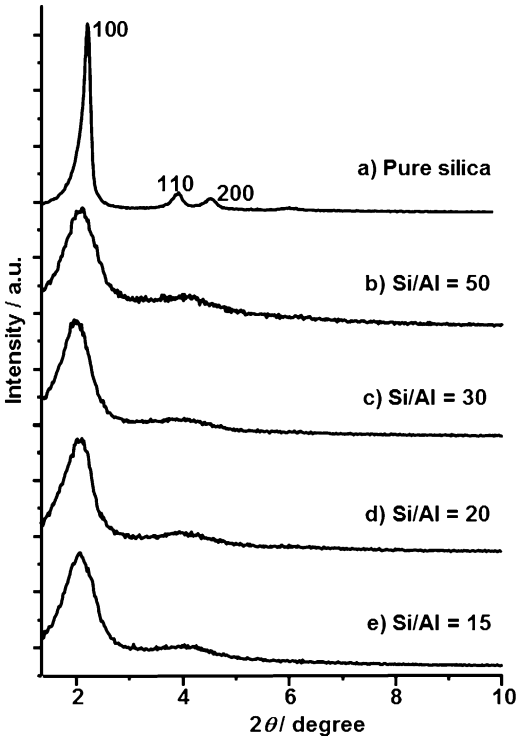

Figure 1. Small-angle XRD patterns of a) [Si]MCM-41 and [Al]MCM-41 with n_{Si}/n_{Al} of b) 50, c) 30, d) 20, and e) 15.

(110), (200), and (210) reflections become small and broad (Figure 1b–e), which hints at a disturbance of this order. This finding as well as the broadening and shift of the (100) reflection to smaller angles that occurs for decreasing n_{Si}/n_{Al} ratios of the [Al]MCM-41 materials is a consequence of the incorporation of Al into the silica framework.[16]

The N_2 adsorption–desorption isotherms and the corresponding Barrett–Joyner–Halenda (BJH) pore size distribution curves of the MCM-41 samples under study are depicted in Figure 2. All samples show type IV isotherms, which indicates a mesoporous structure according to the IUPAC classification.[17] The pore size distributions, evaluated by the BJH model, correspond to narrow and uniform mesopores for all MCM-41 materials under study (inset in Figure 2).

The structural data obtained by XRD and the results of N_2 adsorption are summarized in Table 1. Interestingly, the wall thicknesses (the difference between the average pore size and the unit cell parameter) of the [Al]MCM-41 materials (0.72–1.17 nm) are very similar to those of [Si]MCM-41 in the present study (0.91 nm) and those described in the literature (≈1 nm).[3c] This may indicate that the mechanical strength of the Al-containing MCM-41 materials prepared in this work is comparable to that of conventional MCM-41 materials.

The SEM images of the [Al]MCM-41 samples presented in Figure 3 show a uniform particle shape with particle size in the range of 50 to 200 nm, independent of the Al content. In the transmission electron microscopy (TEM) image of the [Si]MCM-41 material in Figure 4a, a typical regular mesoporous structure with hexagonal pores can be observed clearly.[3c,19] The TEM images of the Al-containing MCM-41 materials shown in

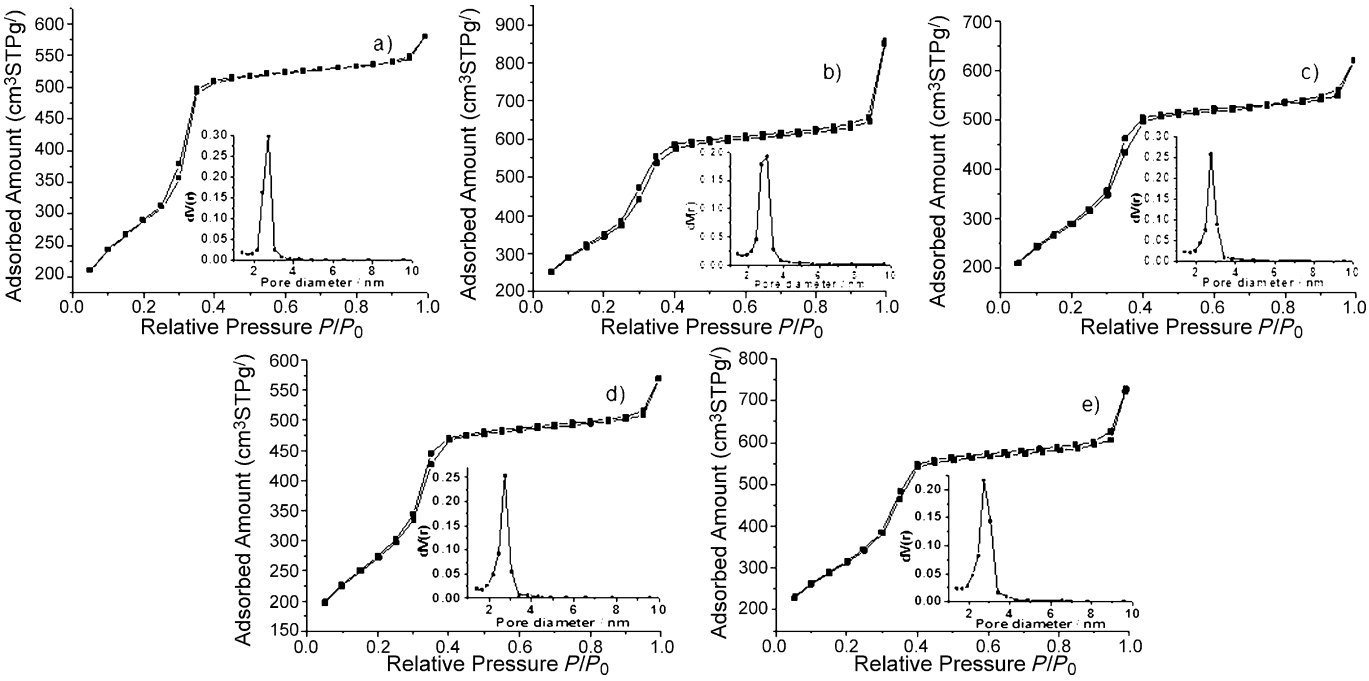

Figure 2. N_2 adsorption–desorption isotherms and pore size distributions of a) [Si]MCM-41 and [Al]MCM-41 with n_{Si}/n_{Al} of b) 50, c) 30, d) 20, and e) 15.

Table 1. Structural and textural properties of the MCM-41 materials under study: $d_{(100)}$ spacing, unit cell parameter a_0, BET surface areas, total pore volume, average pore size, and pore wall thickness.

Sample	$d_{(100)}$ [nm][a]	a_0 [nm][b]	A [$m^2 g^{-1}$][c]	V [$cm^3 g^{-1}$][c]	d [nm][c]	Pore wall thickness [nm]
[Si]MCM-41	3.77	4.35	1042	0.897	3.44	0.91
[Al]MCM-41/50	4.13	4.77	1246	1.324	3.6	1.17
[Al]MCM-41/30	3.84	4.43	1036	0.959	3.6	0.83
[Al]MCM-41/20	3.95	4.56	1005	0.881	3.5	1.06
[Al]MCM-41/15	4.08	4.71	1130	1.127	3.99	0.72
deAl-HY[18]	–	–	671	0.388	1.1	–

[a] The $d_{(100)}$ spacing was calculated by using the $d(100)$ reflection with Bragg's equation ($2d\sin\theta=\lambda$, $\lambda=0.1542$ nm). [b] Hexagonal unit cell parameter $a_0=(2/\sqrt{3})d_{(100)}$, which represents the distance between two neighboring pores. [c] Specific surface area (A), total pore volume (V), and average pore size (d) were determined by N_2 adsorption–desorption isotherms.

Figure 4b–f exhibit more irregular pores, however, only with slight effects on their long-range order as demonstrated by the XRD investigations. The pore size of the material shown in Figure 4c ($\approx$2.8 nm) is smaller than the mean pore size of [Al]MCM-41/50 (3.6 nm), which could be caused by the detection of some small pores that are in the range of the pore size distribution shown in Figure 2b (inset). In comparison with [Al]MCM-41 materials reported in the literature,[8,20] the [Al]MCM-41 materials obtained in this work show typical hexagonal structural properties. The N_2 adsorption–desorption isotherms and BET analysis evidenced the mesoporous structure of these [Al]MCM-41 materials, similar to those reported previously.[8,20] Similar to other [Al]MCM-41 materials,[16] the disturbance of the long-range order of [Al]MCM-41 with increasing Al content was also observed from XRD patterns and TEM images.

Solid-state NMR investigation

^{29}Si magic-angle spinning (MAS) NMR spectroscopy was used to investigate the Si coordination inside the MCM-41 framework. The ^{29}Si MAS NMR spectrum of the [Si]MCM-41 material shown in Figure 5a consists of strong signals at $\delta_{^{29}Si}=-110$ and -101 ppm attributed to Q^4 ($Si(OSi)_4$) and Q^3 ($Si(OSi)_3OH$) species, respectively, and the small hump at $\delta_{^{29}Si}=-92$ ppm is attributed to Q^2 ($Si(OSi)_2(OH)_2$) species. Q^4 species are caused by tetrahedrally coordinated Si atoms, whereas one and two hydroxyl groups are bound to Si atoms that give rise to Q^3 and Q^2 signals, respectively. Generally, the $Q^4/(Q^3+Q^2)$ ratio is used as a measure of the degree of condensation of the silica framework.[21] Upon determining the contents of the different Q^n ($n=0$–4) species by deconvolution and quantitative evaluation of the ^{29}Si MAS NMR spectrum of the [Si]MCM-41 material, a $Q^4/(Q^3+Q^2)$ ratio of 1.4 was obtained, which is similar to that in previous work.[5b,7]

As an example of the Al-containing MCM-41 materials, the ^{29}Si MAS NMR spectrum of [Al]MCM-41/30 is shown in Figure 5b. The strong broadening of the ^{29}Si MAS NMR signals is because of the disturbance of the local Si structure by incorporation of Al into the MCM-41 framework, which agrees with the observations made by XRD and TEM (vide supra). Therefore, in addition to the Q^4, Q^3, and Q^2 signals of Si atoms exclusively coordinated to O–Si– and OH species, a signal from Si atoms coordinated to framework Al atoms (Si(1Al) signals) also

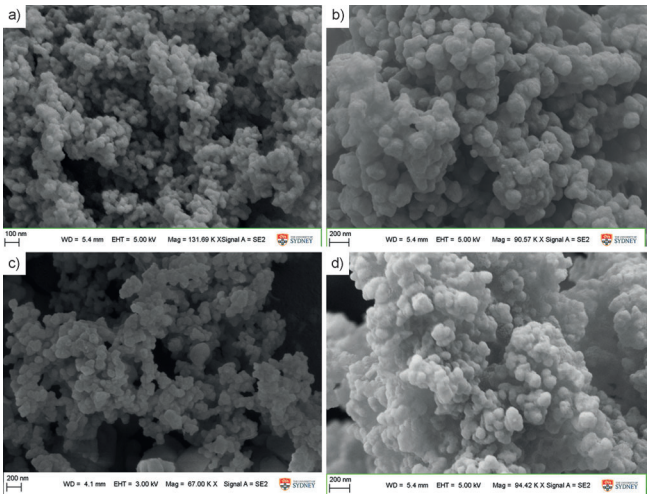

Figure 3. SEM images of [Al]MCM-41 with n_{Si}/n_{Al} of a) 50, b) 30, c) 20, and d) 15.

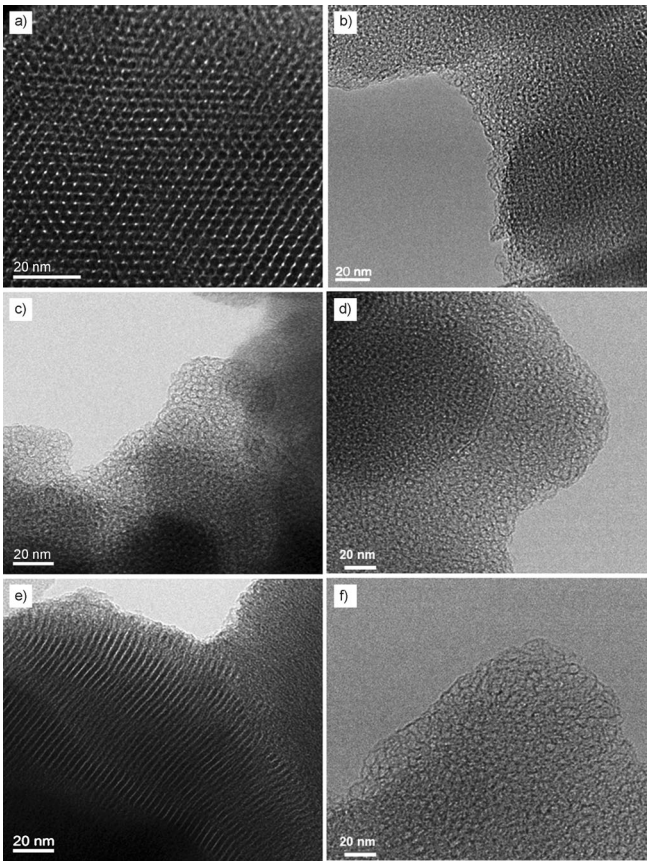

Figure 4. TEM images of a) [Si]MCM-41 and [Al]MCM-41 with n_{Si}/n_{Al} of b) and c) 50, d) 30, e) 20, and f) 15.

contributes to the spectrum shown in Figure 5b. This signal may be the reason for the increase of the signal at approximately −101 ppm (Q^3+Si(1Al)) and the slight shift of the maximum from −110 to −107 ppm in comparison with the spectrum of [Si]MCM-41 shown in Figure 5a.

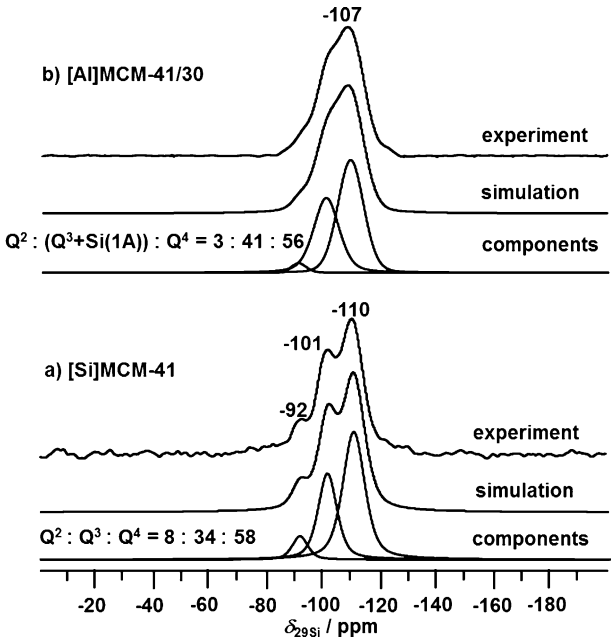

Figure 5. ^{29}Si MAS NMR spectra of a) [Si]MCM-41 and b) [Al]MCM-41 with $n_{Si}/n_{Al} = 30$.

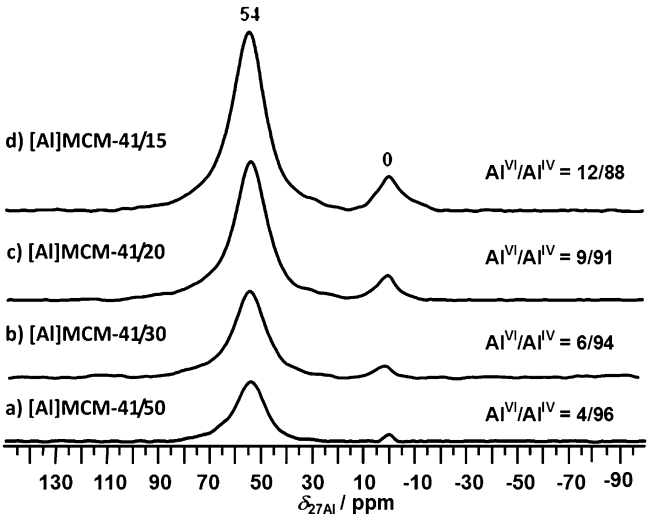

Figure 6. ^{27}Al MAS NMR spectra of [Al]MCM-41 with n_{Si}/n_{Al} of a) 50, b) 30, c) 20, and d) 15.

The ^{27}Al MAS NMR spectra of the [Al]MCM-41 materials shown in Figure 6 are dominated by signals of tetrahedrally coordinated Al^{IV} species (Al(4Si)) at $\delta_{^{27}Al} = 54$ ppm. With the increasing Al content of the synthesis gel that corresponds to a decreasing n_{Si}/n_{Al} ratio from 50 to 15, the Al^{IV} signals become significantly stronger. Hence, a larger number of Al atoms have been incorporated into the silica framework. The weak ^{27}Al MAS NMR signals at $\delta_{^{27}Al} = 0$ ppm are explained by octahedrally coordinated Al^{VI} species that are not incorporated into the silica framework or are located at defect sites.[22]

As discussed for dealuminated zeolites, specific types of octahedrally coordinated extraframework Al species may act as

Lewis acid sites.[18,23] For [Al]MCM-41 materials, the Lewis acidic properties of Al^{VI} species were supported by comparison of the results of FTIR spectroscopy upon adsorption of pyridine as a probe molecule and ^{27}Al MAS NMR spectroscopy.[24] Therefore, the content of the Al^{VI} species in [Al]MCM-41 is interesting for the catalytic properties of these materials. In the present work, an increase the of Al^{VI}/Al^{IV} ratio from 4:96 for [Al]MCM-41/50 to 12:88 for [Al]MCM-41/15 was observed. Clearly, higher Al contents lead to an enhanced probability of Al^{VI} species and possibly to the occurrences of Lewis acid sites. However, the amount of Lewis sites is very low on [Al]MCM-41 materials because of the low content of Al^{VI} species.

Solid-state NMR investigations of various noncrystalline aluminosilicates have demonstrated that tetrahedrally coordinated framework Al^{IV} species in the local structure of SiOH groups can enhance the acid strength of these hydroxyl groups (see Ref. [14b] and references therein). For the application of [Al]MCM-41 materials as catalysts or supports for metal catalysts, therefore, the determination of the density and strength of these acid sites is essential. Suitable methods to characterize these surface sites are ^{1}H and ^{13}C MAS NMR spectroscopy upon adsorption of probe molecules.

The ^{1}H MAS NMR spectra of the dehydrated MCM-41 samples are dominated by strong signals of silanol groups at $\delta_{^{1}H} = 1.8$ ppm (Figure 7, bottom traces).[14b] No low-field signals of bridging SiOHAl groups at 3.6–4.3 ppm,[14b] as typically observed in the spectra of acidic zeolites, were observed in the spectra of [Al]MCM-41. Therefore, the determination of the density of surface OH groups with enhanced acid strength was performed by quantitative ^{1}H MAS NMR spectroscopy of ammonium ions formed upon adsorption of ammonia on dehydrated samples of the MCM-41 materials under study (Figure 7, top traces).[14b,25] In this case, the presence of SiOH groups with an enhanced Brønsted acid strength is indicated by the appearance of an ammonium signal at $\delta_{^{1}H} = 6.6$ ppm. As demonstrated by the spectrum of the ammonia-loaded [Si]MCM-41 material (Figure 7a, top trace), no ammonium ions are formed if no Al is incorporated into the silica framework. For the [Al]MCM-41 materials, however, ^{1}H MAS NMR signals of the ammonium ions increase with increasing Al content (Figure 7b–e, top traces). The quantitative evaluation of these signals gave the densities of SiOH groups with enhanced Brønsted acid strength listed in column 2 of Table 2, which increase from 0.013 mmol g^{-1} for [Al]MCM-41/50 to 0.121 mmol g^{-1} for [Al]MCM-41/15, that is, with increasing Al content. As demonstrated by earlier transfer of population in double resonance (TRAPDOR) experiments,[26] some of the Al species incorporated into the silica framework of MCM-41 materials are located in the vicinity of SiOH groups, which is probably the reason for the enhanced acid strength mentioned above.

As a scale of the acid strength of surface OH groups on solid catalysts, often the adsorbate-induced resonance shift of the NMR signals of probe molecules, such as acetone-2-^{13}C, is used.[14b] In this case, a high adsorbate-induced low-field shift of the ^{13}C MAS NMR signal of acetone-2-^{13}C corresponds a high acid strength of interacting surface OH groups and vice versa. The ^{13}C MAS NMR spectrum of the [Si]MCM-41 sample loaded with acetone-2-^{13}C with a dominant signal at 210 ppm is shown in Figure 8a. The small signals that appear at $\delta_{^{13}C} = 70$–75 ppm in the ^{13}C MAS NMR spectra are probably caused by the conversion of acetone to diacetone alcohol.[27] The signals at approximately 30 and 160 ppm are a result of the nonenriched methyl groups and the enriched C atoms of other acetone condensation products, respectively. The signal at $\delta_{^{13}C} = 210$ ppm agrees very well with that of acetone-2-^{13}C adsorbed on SiOH groups of pure silica.[25] For the Al-containing MCM-41 materials under study, this ^{13}C MAS NMR signal shifted to 212 ppm for [Al]MCM-41/50 and to 213 ppm for [Al]MCM-41/

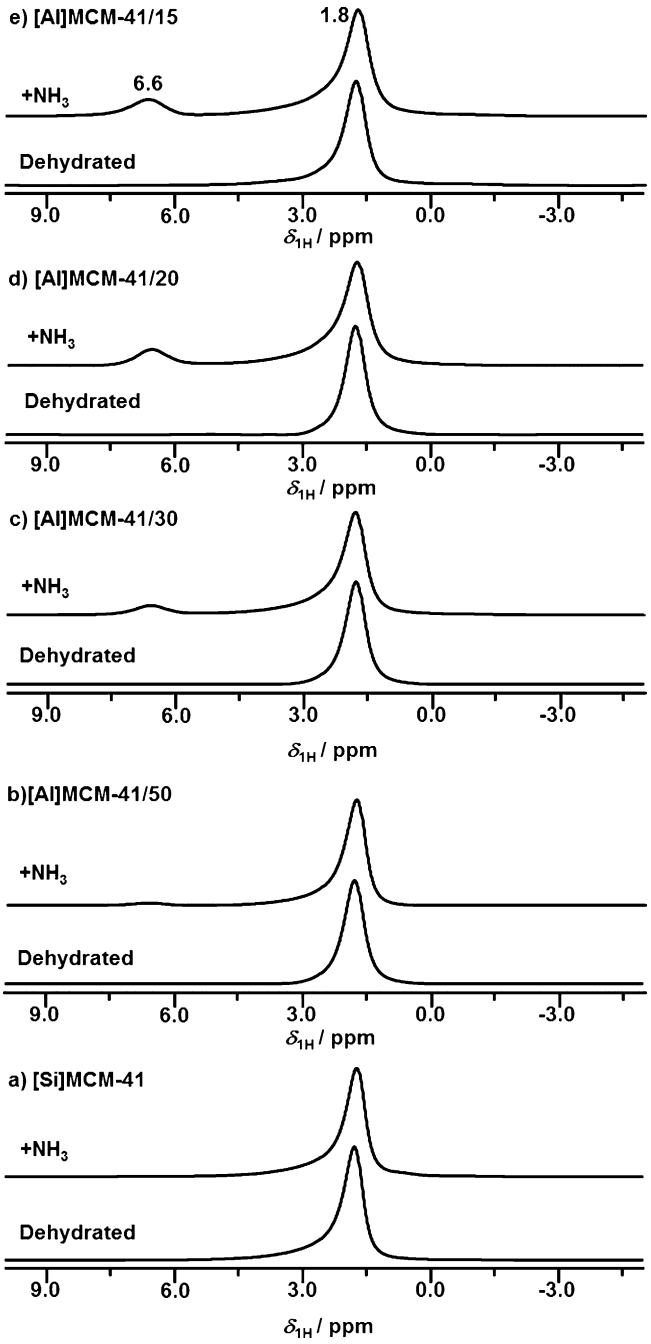

Figure 7. ^{1}H MAS NMR spectra of a) [Si]MCM-41 and [Al]MCM-41 with n_{Si}/n_{Al} of b) 50, c) 30, d) 20, and e) 15.

Table 2. Densities of SiOH groups with enhanced acid strength, contents of octahedrally coordinated Al species, and catalytic performance of the MCM-41 materials with different n_{Si}/n_{Al} ratios in the conversion of PG to EM.

Sample	Amount of Brønsted acid sites [mmol g^{-1}]	Ratio[a] Al^{VI}/Al^{IV}	C_{PG} [%][b]	S_{EM} [mol %][c]	TOF [h^{-1}][d]	S'_{EM} [mol %][e]
[Si]MCM-41	0	0	0	0	0	0
[Al]MCM-41/50	0.013	4/96	77.4	87.5	99.3	98.2
[Al]MCM-41/30	0.07	6/94	87.8	94.2	21	96.5
[Al]MCM-41/20	0.101	9/91	92.5	96.1	15.5	97.5
[Al]MCM-41/15	0.121	12/88	93.4	96.9	13	97.5
deAl-HY[18]	0.865	–	90	90	1.7	90.2

[a] Determined by ^{27}Al MAS NMR spectroscopy. [b] Conversion of PG (0.4 M) in ethanol (1.25 mL) using 50 mg of catalyst at 363 K for 6 h in a batch reactor to yield EM. [c] S_{EM} = selectivity to EM. [d] TOF calculated based on the number of Brønsted acid sites and PG conversion as an averaged value after 6 h reaction. [e] S'_{EM} = selectivity to EM at 50% PG conversion.

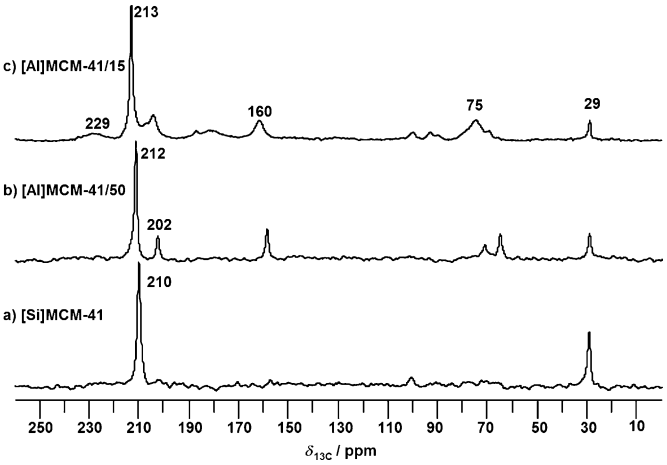

Figure 8. ^{13}C CP MAS NMR spectra of a) [Si]MCM-41 and [Al]MCM-41 materials with n_{Si}/n_{Al} of b) 50 and c) 15.

15. In comparison, the ^{13}C MAS NMR signals of acetone-2-^{13}C adsorbed at acidic bridging OH groups (SiOHAl), for example, of SAPO-type zeolites, zeolite H-ZSM-5, and heteropoly acids were observed at 217, 225, and 235 ppm, respectively.[14b] Hence, the incorporation of Al into the silica network of MCM-41 leads to an enhancement of the acid strength of neighboring SiOH groups, which is, however, weak in comparison with zeolitic bridging OH groups.

The solid-state NMR investigations of the MCM-41 materials under study demonstrate that, as already shown in previous studies,[25] tuning the n_{Si}/n_{Al} ratio leads to changes in the density and acid strength of surface OH groups and the occurrence of a small amount of octahedrally coordinated Al species, which partially may act as Lewis acid sites. These findings are important for the catalytic properties of the [Al]MCM-41 materials under study.

Catalytic conversion of PG

The catalytic performance of the MCM-41 materials was tested for the conversion of PG to EM in ethanol at 363 K. [Si]MCM-41, which is exclusively characterized by nonacidic surface SiOH groups, is not able to convert PG to EM (Table 2, columns 4–6). The total conversion of PG is zero after 6 h. For [Al]MCM-41 materials characterized by SiOH groups with enhanced acid strength, however, the conversion of PG starts immediately even for the [Al]MCM-41/50 material with the lowest Al content. After 6 h, a PG conversion of 77.4% with a selectivity to EM of 87.5% were obtained for this catalyst. Upon further increasing the Al content, which is accompanied by an increase of the density and strength of acid sites, a maximum PG conversion of 93.4% and a selectivity to EM of 96.9% were reached for the [Al]MCM-41/15 material. At a PG conversion of 50%, all [Al]MCM-41 materials had a similar EM selectivity of 96.5–98.2%, which is higher than 90.2% on zeolite deAl-HY.

The turnover frequency (TOF) is often used to evaluate the performance of active sites on the surface of a catalyst during the reaction. The calculated TOFs are summarized in Table 2. If we compare the TOFs of the reactants at the Brønsted acidic surface sites (Table 2), the [Al]MCM-41 materials have an 8–58 times higher activity than zeolite deAl-HY. Clearly, the [Al]MCM-41 materials show a higher activity for PG conversion compared with zeolite deAl-HY, although the zeolite catalyst has a much higher density of Brønsted acid sites with a much higher acid strength.[14b] The possible reason for the different catalytic performances of [Al]MCM-41 materials and the acidic zeolite deAl-HY is that the mesopores (pore size of up to $\approx$4 nm and pore volume of $\approx$1 cm^{3}g^{-1}) of MCM-41 materials offer much better reactant and product diffusion properties than the micropores (pore size of 1.1 nm and pore volume of $\approx$0.4 cm^{3}g^{-1}) of zeolites Y.

In addition, it is important to note that the weak acid sites of [Al]MCM-41 are already able to convert PG to the desired product EM. The much stronger acid strength of the acid sites on zeolite deAl-HY, therefore, can have negative effects, such as hindering the product desorption by strong adsorption on acid sites. If we consider this argument, the differences in the catalytic performances of the [Al]MCM-41 materials under study can also be explained. The slightly higher acid strength of the SiOH groups of [Al]MCM-41/15 in comparison with those of [Al]MCM-41/50 (Figure 8) is not significant for the catalytic activity (TOF). However, the relatively higher content of octahedrally coordinated Al species in [Al]MCM-41/15 (Table 2, column 3) partially act as Lewis acid sites. This may hinder the reactant and product desorption, which leads to an improved PG conversion to EM (Table 2, columns 4 and 5) and, on the other hand, to a lower TOF value (Table 2, column 6).

Conclusions

[Al]MCM-41 acidic catalysts were successfully synthesized at room temperature within 1 h. The obtained [Al]MCM-41 materials are characterized by a highly ordered hexagonal structure with high specific areas of 1005–1246 m^{2}g^{-1} and narrow pore size distributions of 3.44–3.99 nm. ^{29}Si and ^{27}Al magic-angle

spinning (MAS) NMR spectroscopic studies confirmed the well-condensed silica structure and the incorporation of Al atoms into the silica framework. ^{1}H MAS NMR investigations of ammonia-loaded samples showed that the surface of siliceous MCM-41 materials ([Si]MCM-41) is covered by SiOH groups, which are not able to protonate ammonia, that is, of nonacidic properties. The incorporation of Al species into the silica framework of [Al]MCM-41 materials was found to be accompanied by an enhanced acid strength of nearby silanol groups able to protonate ammonia to ammonium. With the increasing Al content of the [Al]MCM-41 materials (n_{Si}/n_{Al} ratios of 50 to 15), the density of the SiOH groups with enhanced Brønsted acid strength increased from 0.013 to 0.121 mmol g^{-1}. Using acetone-2-^{13}C as a probe molecule for ^{13}C MAS NMR investigations of these surface sites, the enhanced acid strength of SiOH groups in [Al]MCM-41 materials could be supported but was found to be significantly lower than that of bridging OH groups (SiOHAl) in acidic zeolites.

In the catalytic studies, [Si]MCM-41 was not able to initiate the PG conversion within a reaction time of 6 h, but the [Al]MCM-41 materials could immediately start the PG conversion to EM. The turnover frequencies (TOFs) of the reactants at the catalytically active surface sites of the [Al]MCM-41 materials hint at their 8–58 times higher activity than that of a dealuminated zeolite Y used as a reference catalyst. The different catalytic performances of the [Al]MCM-41 materials and the zeolite Y is explained by the large size of the mesopores of the MCM-41 materials, which offers much better reactant and product diffusion properties than the micropores of zeolite Y.

Experimental Section

Catalyst preparation

All chemicals used for the MCM-41 synthesis, such as an ammonium hydroxide solution (28% NH_3 in H_2O), tetraethylorthosilicate (TEOS, >98%), hexadecyltrimethylammoniumchloride solution (CTACl, purum, ≈25% in H_2O), and aluminum sulfate octadecahydrate (>98%) were obtained from Sigma–Aldrich. For the typical preparation of [Si]MCM-41 material, CTACl was mixed with an ammonium hydroxide solution and TEOS in a volume ratio of 1:1:1 in demineralized water (500 mL) and stirred at RT to form a white gel. For the synthesis of [Al]MCM-41 materials with different n_{Si}/n_{Al} ratios, calculated amounts of aluminum sulfate were added to the above gels. The obtained gels were completely mixed with vigorous stirring for 1 h. The resulting solids were collected by filtration, washed with distilled water, and then in an oven at 353 K. Finally, the obtained MCM-41 materials were calcined at 823 K with a heating rate of 1 K min^{-1} in the presence of static air for 6 h. The nomenclature of [Al]MCM-41 is defined as [Al]MCM-41/*x*, where *x* represents the n_{Si}/n_{Al} ratios of 15, 20, 30, and 50. Dealuminated zeolite deAl-HY (n_{Si}/n_{Al} = 5.4), used as a reference catalyst, was obtained by steaming a zeolite H-Y (n_{Si}/n_{Al} = 2.7) at 748 K for 2.5 h.[18]

Characterization of textural and morphological properties

Small-angle XRD, SEM, and TEM were employed to characterize the structure and morphology of the MCM-41 materials. The XRD studies were performed by using a Siemens D5000 with CuK_α radiation in the range of 1.5–10° with scanning steps of 0.02°. SEM images were recorded by using a FESEM, Zeiss Ultra+. TEM images were obtained by using a Philips CM120 BioFilter with samples that were mounted on a carbon-coated copper grid by drying a droplet of a suspension of the ground sample in ethanol. The surface area, average pore size, and total pore volume of the MCM-41 materials were determined by N_2 adsorption–desorption isotherms by using an Autosorb IQ-C system. Each sample (50 mg) was degassed at 423 K for 12 h under vacuum before the measurements and then recorded at 77 K.

Solid-state NMR investigations

For the ^{27}Al and ^{29}Si MAS NMR investigations, all samples were fully hydrated by exposure to the saturated vapor of a $Ca(NO_3)_2$ solution at ambient temperature overnight in a desiccator. Before the ^{1}H and ^{13}C MAS NMR experiments, the samples in glass tubes were dehydrated at 723 K for 12 h at a pressure lower than 10^{-2} bar. These dehydrated samples were sealed in the glass tubes or directly loaded with ammonia or acetone-2-^{13}C (99.5% ^{13}C-enriched, Sigma–Aldrich) by using a vacuum line. The loaded samples were evacuated at 393 K for 1 h (for ammonia) or at RT for 2 h (for acetone) to remove weakly physisorbed molecules. Subsequently, the samples were transferred into the MAS NMR rotors under dry N_2 inside a glove box.

^{1}H, ^{27}Al, and ^{13}C MAS NMR spectroscopy was performed by using a Bruker Avance III 400 WB spectrometer at resonance frequencies of 400.1, 104.3, and 100.6 MHz, respectively, with a sample spinning rate of 8 kHz using 4 mm MAS rotors. The spectra were recorded after single-pulse $\pi/2$ and $\pi/6$ excitation with repetition times of 20 and 0.5 s for the ^{1}H and ^{27}Al nuclei, respectively. Quantitative ^{1}H MAS NMR spectroscopy was performed by using a zeolite H,Na-Y (35% ion exchanged) as an external intensity standard. ^{13}C cross-polarization (CP) MAS NMR spectra were recorded with a contact time of 4 ms and a repetition time of 4 s. ^{29}Si MAS NMR spectra were recorded on the same spectrometer at a resonance frequency of 79.5 MHz with a sample spinning rate of 4 kHz using a 7 mm MAS rotor. For the ^{29}Si MAS NMR spectroscopic studies, single-pulse $\pi/2$ excitation, high-power proton decoupling, and a recycle delay of 20 s were applied.

Catalytic reaction

The conversion of PG (Sigma–Aldrich, >97%) to EM was used to study the catalytic performance of the MCM-41 materials. Dealuminated zeolite deAl-HY was used as a reference catalyst. This has the same catalytic properties as dealuminated zeolite HY reported in the literature as the best catalyst for this reaction.[12c] Therefore, using zeolite deAl-HY and the mesoporous [Al]MCM-41 material under the same reaction conditions is a better way to compare their catalytic properties than to compare with the reported dealuminated zeolite HY. The MCM-41 catalyst (0.05 g) or zeolite deAl-HY was employed and activated in a U-tube with N_2 (50 mL min^{-1}) at 723 K overnight. After cooling the catalyst under flowing N_2 gas, it was transferred into a glass reactor with a volume of 15 mL. Subsequently, an ethanol solution (1.25 mL) that contained PG (0.4 M) and octane (0.05 M; as the GC internal standard) was added to the glass reactor filled with activated catalyst. The reaction was performed in the tightly closed glass reactor, which was heated in a stirred oil bath at 363 K for 6 h. The reaction products were analyzed by using GC (Shimadzu GCMS-QP2010 Ultra equipped with a Rtx-5 MS, 30 m×0.25 mm×0.25 μm) with MS detection and GC (25QC3/BP1, 25 m×0.32 mm×5 μm) with flame ionization detec-

tion. The selectivity to specific products i (S_i) was calculated by using Equation (1):

$$S_i\,[\%] = 100 \times [i]/([PG]_0 - [PG]) \quad (1)$$

in which [i] is the molar concentration of the product i and $[PG]_0$ and [PG] correspond to the molar concentrations of PG before and after reaction, respectively.

Acknowledgements

This work was supported by the Early Career Research Scheme and the Major Equipment Scheme from the University of Sydney. M.H. thanks the Deutsche Forschungsgemeinschaft and the Baden-Württemberg Stiftung for financial support.

Keywords: acidity · aluminum · heterogeneous catalysis · mesoporous materials · nmr spectroscopy

[1] a) J. S. Beck, J. C. Vartuli, W. J. Roth, M. E. Leonowicz, C. T. Kresge, K. D. Schmitt, C. T. W. Chu, D. H. Olson, E. W. Sheppard, S. B. McCullen, J. B. Higgins, J. L. Schlenker, *J. Am. Chem. Soc.* **1992**, *114*, 10834; b) C. T. Kresge, M. E. Leonowicz, W. J. Roth, J. C. Vartuli, J. S. Beck, *Nature* **1992**, *359*, 710.

[2] a) G. J. D. Soler-illia, C. Sanchez, B. Lebeau, J. Patarin, *Chem. Rev.* **2002**, *102*, 4093; b) A. Corma, *Chem. Rev.* **1997**, *97*, 2373; c) A. Firouzi, D. Kumar, L. M. Bull, T. Besier, P. Sieger, Q. Huo, S. A. Walker, J. A. Zasadzinski, C. Glinka, J. Nicol, D. Margolese, G. D. Stucky, B. F. Chmelka, *Science* **1995**, *267*, 1138; d) J. Patarin, B. Lebeau, R. Zana, *Curr. Opin. Colloid Interface Sci.* **2002**, *7*, 107.

[3] a) K. Lin, P. P. Pescarmona, H. Vandepitte, D. Liang, G. Van Tendeloo, P. A. Jacobs, *J. Catal.* **2008**, *254*, 64; b) A. Pourahmad, S. Sohrabnezhad, *J. Alloys Compd.* **2009**, *484*, 314; c) Q. Cai, Z. S. Luo, W. Q. Pang, Y. W. Fan, X. H. Chen, F. Z. Cui, *Chem. Mater.* **2001**, *13*, 258; d) M. Broyer, S. Valange, J. P. Bellat, O. Bertrand, G. Weber, Z. Gabelica, *Langmuir* **2002**, *18*, 5083; e) U. Ciesla, F. Schüth, *Microporous Mesoporous Mater.* **1999**, *27*, 131; f) Q. Cai, W. Y. Lin, F. S. Xiao, W. Q. Pang, X. H. Chen, B. S. Zou, *Microporous Mesoporous Mater.* **1999**, *32*, 1; g) P. Ågren, M. Linden, J. B. Rosenholm, R. Schwarzenbacher, M. Kriechbaum, H. Amenitsch, P. Laggner, J. Blanchard, F. Schüth, *J. Phys. Chem. B* **1999**, *103*, 5943; h) M. Grün, I. Lauer, K. K. Unger, *Adv. Mater.* **1997**, *9*, 254.

[4] a) M. Grün, K. K. Unger, A. Matsumoto, K. Tsutsumi, *Microporous Mesoporous Mater.* **1999**, *27*, 207; b) P. Verlooy, A. Aerts, O. I. Lebedev, G. Van Tendeloo, C. Kirschhock, J. A. Martens, *Chem. Commun.* **2009**, 4287; c) Y. M. Setoguchi, Y. Teraoka, I. Moriguchi, S. Kagawa, N. Tomonaga, A. Yasutake, J. Izumi, *J. Porous Mater.* **1997**, *4*, 129; d) F. J. Romero, C. Jiménez, I. Huc, R. Oda, *Microporous Mesoporous Mater.* **2004**, *69*, 43.

[5] a) G. Lelong, S. Bhattacharyya, S. Kline, T. Cacciaguerra, M. A. Gonzalez, M. L. Saboungi, *J. Phys. Chem. C* **2008**, *112*, 10674; b) S. N. Che, S. Y. Lim, M. Kaneda, H. Yoshitake, O. Terasaki, T. Tatsumi, *J. Am. Chem. Soc.* **2002**, *124*, 13962.

[6] Q. S. Huo, J. L. Feng, F. Schüth, G. D. Stucky, *Chem. Mater.* **1997**, *9*, 14.

[7] a) K. F. Lin, P. P. Pescarmona, K. Houthoofd, D. D. Liang, G. Van Tendeloo, P. A. Jacobs, *J. Catal.* **2009**, *263*, 75.

[8] a) A. Matsumoto, H. Chen, K. Tsutsumi, M. Grun, K. Unger, *Microporous Mesoporous Mater.* **1999**, *32*, 55; b) K. M. Parida, D. Rath, *J. Colloid Interface Sci.* **2009**, *340*, 209.

[9] K. Xia, R. Z. Ferguson, M. Losier, N. Tchoukanova, R. Bruening, Y. Djaoued, *J. Hazard. Mater.* **2010**, *183*, 554.

[10] a) M. Abdollahi-Alibeik, M. Pouriayevali, *Catal. Commun.* **2012**, *22*, 13; b) M. S. Sadjadi, N. Farhadyar, K. Zare, *Superlattices Microstruct.* **2009**, *46*, 266.

[11] a) A. Corma, V. Fornes, M. T. Navarro, J. Perezpariente, *J. Catal.* **1994**, *148*, 569; b) A. Palani, A. Pandurangan, *J. Mol. Catal. A: Chem.* **2005**, *226*, 129.

[12] a) F. de Clippel, M. Dusselier, R. Van Rompaey, P. Vanelderen, J. Dijkmans, E. Makshina, L. Giebeler, S. Oswald, G. V. Baron, J. F. M. Denayer, P. P. Pescarmona, P. A. Jacobs, B. F. Sels, *J. Am. Chem. Soc.* **2012**, *134*, 10089; b) L. Li, C. Stroobants, K. F. Lin, P. A. Jacobs, B. F. Sels, P. P. Pescarmona, *Green Chem.* **2011**, *13*, 1175; c) P. P. Pescarmona, K. P. F. Janssen, C. Delaet, C. Stroobants, K. Houthoofd, A. Philippaerts, C. De Jonghe, J. S. Paul, P. A. Jacobs, B. F. Sels, *Green Chem.* **2010**, *12*, 1083.

[13] a) G. M. Coppola, H. F. Schuster, *α-Hydroxy Acids in Enantioselective Synthesis* Wiley-VCH, Weinheim, **1997**; b) A. Corma, S. Iborra, A. Velty, *Chem. Rev.* **2007**, *107*, 2411.

[14] a) M. Hunger, U. Schenk, M. Breuninger, R. Glaser, J. Weitkamp, *Microporous Mesoporous Mater.* **1999**, *27*, 261; b) Y. Jiang, J. Huang, W. Dai, M. Hunger, *Solid State Nucl. Magn. Reson.* **2011**, *39*, 116.

[15] N. T. Mathew, S. Khaire, S. Mayadevi, R. Jha, S. Sivasanker, *J. Catal.* **2005**, *229*, 105.

[16] a) Z. H. Luan, C. F. Cheng, W. Z. Zhou, J. Klinowski, *J. Phys. Chem.* **1995**, *99*, 1018; b) X. Y. Chen, L. M. Huang, G. Z. Ding, Q. Z. Li, *Catal. Lett.* **1997**, *44*, 123.

[17] K. S. W. Sing, D. H. Everett, R. A. W. Haul, L. Moscou, R. A. Pierotti, J. Rouquerol, T. Siemieniewska, *Pure Appl. Chem.* **1985**, *57*, 603.

[18] J. Huang, Y. J. Jiang, V. R. R. Marthala, Y. S. Ooi, M. Hunger, *ChemPhysChem* **2008**, *9*, 1107.

[19] C.-Y. Chen, H.-X. Li, M. E. Davis, *Microporous Mater.* **1993**, *2*, 17.

[20] a) K. U. Nandhini, B. Arabindoo, N. Palanichamy, V. Murugesan, *J. Mol. Catal. A: Chem.* **2006**, *243*, 183; b) S. Udayakumar, A. Pandurangan, P. K. Sinha, *Appl. Catal. A* **2005**, *287*, 116; c) F. González, C. Pesquera, A. Perdigon, C. Blanco, *Appl. Surf. Sci.* **2009**, *255*, 7825; d) L. Y. Chen, Z. Ping, G. K. Chuah, S. Jaenicke, G. Simon, *Microporous Mesoporous Mater.* **1999**, *27*, 231; e) B. Lindlar, A. Kogelbauer, R. Prins, *Microporous Mesoporous Mater.* **2000**, *38*, 167; f) H. M. Yang, Y. H. Deng, C. F. Du, S. M. Jin, *Appl. Clay Sci.* **2010**, *47*, 351; g) Z. Q. Zhang, J. Xiao, L. Dai, Y. Y. Wang, D. Q. Wang, X. M. Liu, Z. F. Yan, *J. Porous Mater.* **2012**, *19*, 473.

[21] S. Vetrivel, C.-T. Chen, H.-M. Kao, *New J. Chem.* **2010**, *34*, 2109.

[22] Z. H. Luan, C. F. Cheng, H. Y. He, J. Klinowski, *J. Phys. Chem.* **1995**, *99*, 10590.

[23] a) R. Rachwalik, Z. Olejniczak, J. Jiao, J. Huang, M. Hunger, B. Sulikowski, *J. Catal.* **2007**, *252*, 161; b) G. H. Kuehl, H. K. C. Timken, *Microporous Mesoporous Mater.* **2000**, *35–36*, 521.

[24] a) A. N. Ko, C. C. Hung, C. W. Chen, K. H. Ouyang, *Catal. Lett.* **2001**, *71*, 219; b) R. Baran, Y. Millot, T. Onfroy, J. M. Krafft, S. Dzwigaj, *Microporous Mesoporous Mater.* **2012**, *163*, 122.

[25] J. Huang, N. van Vegten, Y. Jiang, M. Hunger, A. Baiker, *Angew. Chem.* **2010**, *122*, 7942; *Angew. Chem. Int. Ed.* **2010**, *49*, 7776.

[26] a) M. Xu, W. Wang, M. Seiler, A. Buchholz, M. Hunger, *J. Phys. Chem. B* **2002**, *106*, 3202; b) Q. Luo, F. Deng, Z. Y. Yuan, J. Yang, M. J. Zhang, Y. Yue, C. H. Ye, *J. Phys. Chem. B* **2003**, *107*, 2435.

[27] A. I. Biaglow, R. J. Gorte, D. White, *J. Catal.* **1994**, *150*, 221.

Received: May 16, 2013
Revised: June 25, 2013
Published online on ■■ ■■, 0000

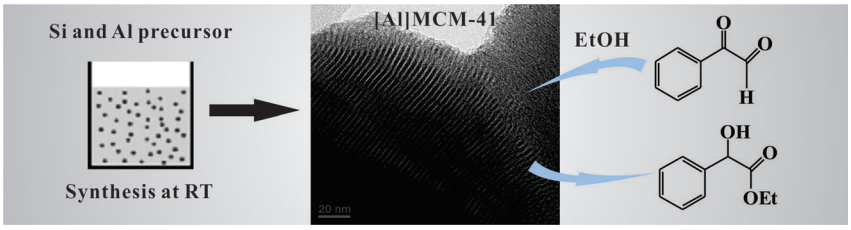

Mesopores flex their catalytic muscles: Mesoporous [Al]MCM-41 materials with n_{Si}/n_{Al} ratios of 15 to 50 suitable for the direct catalytic conversion of phenylglyoxal to ethylmandelate were successfully synthesized at room temperature within 1 h.

Z. Wang, Y. Jiang, R. Rachwalik, Z. Liu, J. Shi, M. Hunger, J. Huang**

■■ – ■■

One-Step Room-Temperature Synthesis of [Al]MCM-41 Materials for the Catalytic Conversion of Phenylglyoxal to Ethylmandelate